ISSN 2616-5880 Vol. 4, Issue 3: 1-14, DOI: 10.25236/AJMC.2023.040301

Preparation of modified TiO_2 and its photocatalytic properties

Ting Liu[a,*]

School of Materials Science and Engineering, Chongqing Jiaotong University, Chongqing, China
[a]*1581788875@qq.com*
[*]*Corresponding author*

Abstract: *In this chapter, tetrabutyl titanate was used as the titanium source, and the photocatalytic performance of commercial TiO_2 and self-made TiO_2 was compared by sol-gel method. Since ready-made commercial TiO_2 is not easy to be doped and modified, this chapter also performs alkali solution surface modification at the same time as self-made TiO_2 (that is, the TiO_2 to be modified is immersed in alkali solution at different pH values and then dried), and the photocatalytic performance of the two before and after the surface modification of alkali solution is compared. In order to improve the photocatalytic performance of self-made TiO_2, this chapter modifies the iron doping of self-made TiO_2 during the preparation process to enhance its photocatalytic performance. After iron doping modification of TiO_2, in order to further improve its performance, the modified sample was modified with alkali solution surface. In this paper, the microscopic characterization and nitrogen and oxygen catalytic performance tests of each sample were carried out, and the results showed that the photocatalytic performance of self-prepared TiO_2 was significantly better than that of commercial TiO_2. Among the TiO_2 modified by different pH solutions, the catalytic performance was the best at pH 11.5, and the photocatalytic performance of Fe-doped TiO_2 was also improved to varying degrees compared with pure TiO_2, among which Fe doping 0.5% contributed the most to the photocatalytic performance. After the surface modification of Fe (0.5%)-TiO_2 with the best doping amount by alkali solution, the photocatalytic performance was also improved.*

Keywords: *TiO_2, Doped, Surface modification, Photocatalytic*

1. Introduction

In recent years, the rapid development of industrialization has led to a sharp increase in the discharge of global industrial waste gas and wastewater. Natural waters contain pollutants such as heavy metals and organic substances emitted by humans [1]; Air pollution is also serious, acid rain, smog and other meteorological frequent [2], causing great harm and loss to human health [3] and social economy.

As a nanoscale technology, photocatalytic technology was born at the end of the 20th century, photocatalyst is a substance with catalytic effect, which can occur photocatalytic reaction under light [4]. It can purify organic pollutants and heavy metal ions in water under natural light [5]; Photocatalytic purification of air pollutants, such as converting toxic nitric oxide into non-toxic nitrogen dioxide under photocatalysis, purifying indoor formaldehyde gas, etc.[6]. Titanium dioxide is a common semiconductor photocatalyst, which under the excitation of light, electrons in molecular orbitals on the valence band transition to the conduction band, so that photogenerated holes and photogenerated electrons are formed on the valence band and conduction band, respectively. Photogenerated holes and photogenerated electrons undergo redox reactions with the exposed pollutants, thereby decomposing the pollutants into harmless products. In the existing research reports, titanium dioxide has a significant effect on photocatalytic degradation of automobile exhaust, purification of organic matter, heavy metal ions and other aspects.

TiO_2 has been used in photocatalysis, medical, new energy, chemical and many other fields, so commercial TiO_2 is very common in the market, and purchasing off-the-shelf commercial TiO_2 has become a very time-saving and economical choice. However, because commercial TiO_2 has a variety of excellent properties and is widely used, its photocatalytic performance is relatively not so prominent. Studies have shown [7] that the aging time, calcination temperature and annealing temperature during the preparation of TiO_2 will have a great impact on its structure and properties. The precursor is

ISSN 2616-5880 Vol. 4, Issue 3: 1-14, DOI: 10.25236/AJMC.2023.040301

selected for the preparation of TiO_2 by itself, which can flexibly control the performance required for process preparation. In previous studies, due to the influence of its own band gap and other factors [8], the photocatalytic performance of TiO_2 itself is poor, so it needs to be modified. Single modifications, such as ion doping, construction of heterojunctions, surface modification, etc. [9], are very common modification methods. Ion doping can change the TiO_2 band gap and expand its light absorption range. The construction of heterojunctions can enhance the transfer efficiency of photogenerated carriers and effectively reduce the recombination rate of electron-hole pairs. Surface modification is to treat the surface of the material accordingly, so as to enhance its specific surface area, light absorption capacity, oxygen adsorption capacity, etc. In addition, there are many researchers who have diversified its modifications, which further improves its performance.

2. Experimental programs

2.1. Materials

Ferric nitrate nonahydrate and commercial TiO_2 were purchased from Shanghai Maclin Biochemical Technology Co., Ltd., tetrabutyl titanate, glacial acetic acid and absolute ethanol were purchased from Chengdu Cologne Chemical Co., Ltd., and deionized water was prepared in the laboratory.

2.2. Materials preparation

2.2.1. Preparation of commercial TiO_2 surface modified by alkali solution

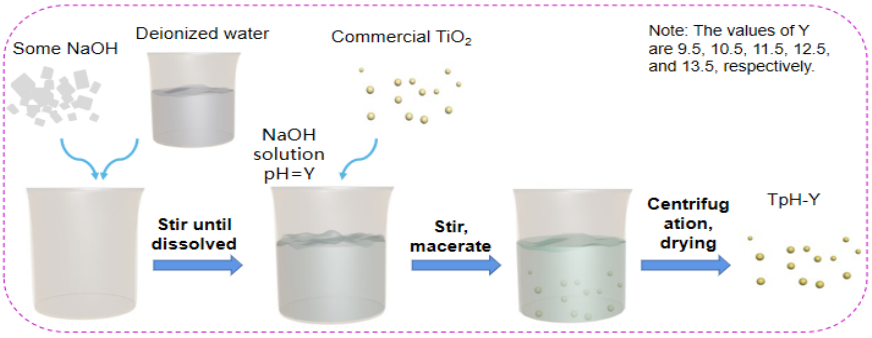

Figure 1: Preparation flow chart of commercial TiO_2 for surface modification of alkali solution.

In Figure 1, according to the standard method of alkali solution preparation, NaOH is used as the raw material of alkali solution, and pH meter is used as the pH measurement tool to prepare alkali solutions with pH of 9.5, 10.5, 11.5, 12.5 and 13.5 respectively, and then take the same amount of commercial TiO_2 powder, add it into the alkali solution, stir it evenly and soak it for 24h, then centrifuge the mixed alkali solution, and finally dry the impregnated commercial TiO_2 powder. In order to compare the performance changes of commercial TiO_2 under alkali solution treatment, a control group with pH 7 (the impregnation solution is deionized water) was prepared at the same time. All samples are named as TpH-7, TpH-10, TpH-11, TpH-12, TpH-13 and TpH-14 according to their pH values.

2.2.2. Preparation of self-made TiO_2 for surface modification of alkali solution

In Figure 2, in order to explore the difference of photocatalytic performance between self-made TiO_2 and commercial TiO_2, and the performance change of both after modification by alkali solution. In this section of the experiment, tetrabutyl titanate was used as the Ti source to synthesize self-made TiO_2 by the sol gel method. The specific experimental steps are as follows: as shown in Figure 2, measure 16ml of tetrabutyl titanate and 40ml of anhydrous ethanol respectively into a beaker, put them into a magnetic rotor, and then continuously stir them on a magnetic stirrer for 30min, and name the mixed solution at this time as solution A. Then measure 4 ml of glacial acetic acid, 3 ml of deionized water and 12 ml of anhydrous ethanol respectively and pour them into the beaker, mix and shake them, and then name them solution B. While solution A is still stirring, drop solution B into solution A with a rubber tip dropper at a rate of about 2 drops per second, and then continue stirring until the mixture is gel like. The prepared gel was aged at room temperature for 24h, and then the gel was baked into dry gel in an oven at 80 ℃. Grind dry gel into powder with mortar, put it into a covered crucible, and put it

ISSN 2616-5880 Vol. 4, Issue 3: 1-14, DOI: 10.25236/AJMC.2023.040301

into a muffle furnace for burning. The calcination conditions are as follows: raise the temperature from room temperature to 400 ℃ at a heating rate of 10 ℃/min, and then keep it for 2h. After the muffle furnace is lowered to room temperature, take out the sample, wash it with deionized water for three times, and then dry it in the oven at 80 ℃ for 8 hours.

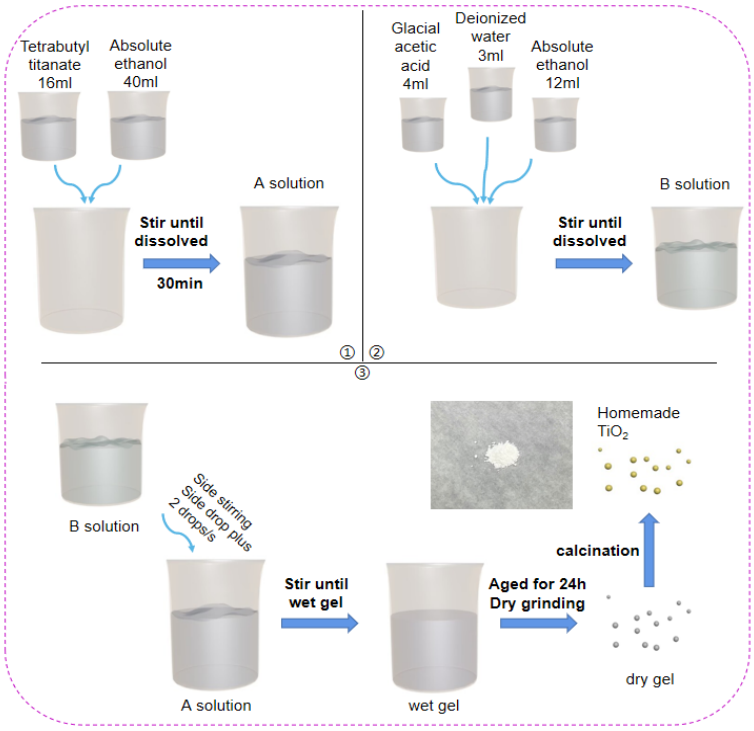

Figure 2: Preparation flow chart of self-made TiO_2.

In order to modify the surface of the alkali solution of the sample, the obtained sample is modified with the alkali solution of the self-made TiO_2 sample according to the method in 2.1.1 in the previous section. The modified sample is named as TiO_2 - 7, TiO_2 - 9.5, TiO_2 - 10.5, TiO_2 - 11.5, TiO_2 - 12.5 and TiO_2 - 13.5 according to the pH value of the alkali solution.

2.2.3. Preparation of Fe-doped TiO_2

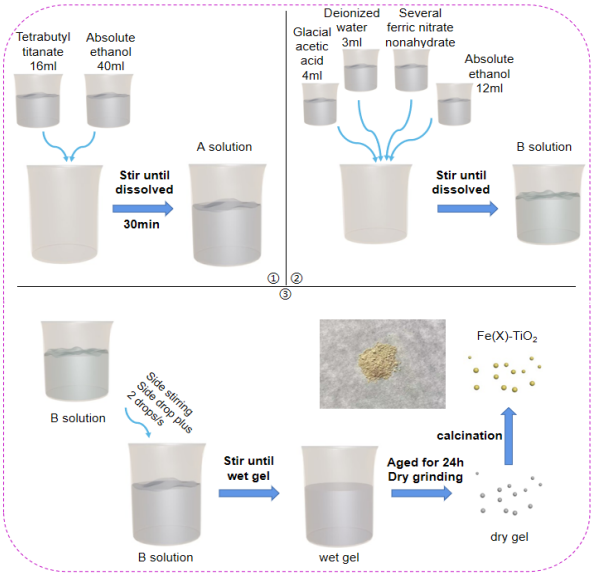

Figure 3: Preparation flow chart of Fe-doped TiO_2.

In Figure 3, in this section of experiment, Fe (X) - TiO_2 (X is the molar ratio of Fe atom to Ti atom) was synthesized by sol gel method with ferric nitrate and tetrabutyl titanate as Fe source and Ti source

ISSN 2616-5880 Vol. 4, Issue 3: 1-14, DOI: 10.25236/AJMC.2023.040301

respectively. Fe (X) - TiO_2 with different Fe doping ratios was prepared by using Fe/Ti molar ratios of 0%, 0.2%, 0.5%, 1% and 1.5% respectively.

Specific experimental steps: Take 16ml of tetrabutyl titanate and 40ml of anhydrous ethanol respectively into the beaker, add the magnetic rotor and stir for 30min, which is solution A. Then take 4 ml of glacial acetic acid, 3 ml of deionized water, 12 ml of anhydrous ethanol and iron nitrate in the corresponding Fe/Ti molar ratio, mix and shake, and record as solution B. While solution A is still stirring, drop solution B into solution A with a rubber tip dropper at a rate of about 2 drops per second, and continue stirring until the mixed solution is in the form of gel. The prepared gel was aged at room temperature for 24h, and then the gel was baked into dry gel in an oven at 80 ℃. Grind the dry gel into powder, put it into a covered crucible, and put it into a muffle furnace for calcination. The calcination conditions are as follows: raise the temperature from room temperature to 400 ℃ at a heating rate of 10 ℃/min, and then keep it for 2h. After the muffle furnace is lowered to room temperature, take out the sample, wash it with deionized water for three times, and then dry it in the oven at 80 ℃ for 8 hours. They are named as: Fe (0%) - TiO_2, Fe (0.2%) - TiO_2, Fe (0.5%) - TiO_2, Fe (1%) - TiO_2, and Fe (1.5%) - TiO_2.

2.2.4. Preparation of surface modified Fe-TiO_2 with alkali solution

Refer to the method in 2.1.1 in the previous section, take the same amount of Fe (0.5%) - TiO_2 sample, immerse it in the alkali solution with pH of 9.5, 10.5, 11.5, 12.5 and 13.5 respectively, and obtain the test sample after the immersion, centrifugal drying and other experimental steps. According to the pH value of the alkali solution, the obtained samples were named as: Fe (0.5%) TiO_2-9.5, Fe (0.5%) TiO_2-10.5, Fe (0.5%) TiO_2-11.5, Fe (0.5%) TiO_2-12.5, and Fe (0.5%) TiO_2-13.5.

3. Results and discussion

3.1. Material characterization

3.1.1. Scanning electron microscope(SEM)

In order to study the effect of modification on TiO_2 morphology, a series of samples were tested by SEM in this section. Figure 4 is the scanning electron microscope micrograph of TiO_2 samples before and after modification. Figure 4(a) and Figure 4(b) are the micrograph of commercial TiO_2 (TpH-7) before modification and commercial TiO_2 (TpH-11.5) after surface modification with alkali solution, respectively. From Figure 4 (a), it can be seen that the nanoparticles of TpH-7 are nearly spherical, with uniform size and distribution; It can be seen from Figure 4(b) that the morphology of commercial TiO_2 (TpH-11.5) has not changed significantly after the surface modification of alkali solution. The particle size and morphology, particle uniformity and dispersion are consistent with those of TpH-7 group samples in Figure 4 (a). This shows that the surface modification of alkali solution will not have a significant impact on the morphology of commercial TiO_2.

Figure 4(c) and Figure 4(d) are the micrographs of self-made TiO_2 (TiO_2-7) and self-made TiO_2 (TiO_2 - 11.5) after surface modification of alkali solution, respectively. Comparing the two figures, it can be found that the micrographs of self-made TiO_2 before and after surface modification of alkali solution have not changed, and the particle size is consistent and evenly distributed, which indicates that the surface modification of alkali solution has no effect on the micrographs of self-made TiO_2. However, comparing Figure 4(a) with Figure 4(c), it can be found that under the same multiple, the average particle size of commercial TiO_2 nanoparticles is about 50 nm, and the average particle size of self-made TiO_2 nanoparticles is about 20 nm. Because titanium dioxide has a large specific surface area when its particle size is small, it can absorb more sunlight, thus improving the photocatalytic performance. Figure 4(e) and Figure 4(f) are the morphologies of self-made TiO_2 (Fe (0%) - TiO_2) and Fe-doped self-made TiO_2 (Fe (0.5%) - TiO_2), respectively. It can be found that there is no significant difference in the size and distribution of the nanoparticles in the two figures, which indicates that Fe-doped modification will not affect the morphology of self-made TiO_2. Figure 4(g) and Figure 4(h) show the morphology of Fe-doped self-made TiO_2 (Fe (0.5%) - TiO_2) and alkali solution modified Fe-doped TiO_2 (Fe (0.5%) TiO_2-11.5). It can also be found that the surface modification of alkali solution will not change the morphology of Fe (0.5%) - TiO_2.

ISSN 2616-5880 Vol. 4, Issue 3: 1-14, DOI: 10.25236/AJMC.2023.040301

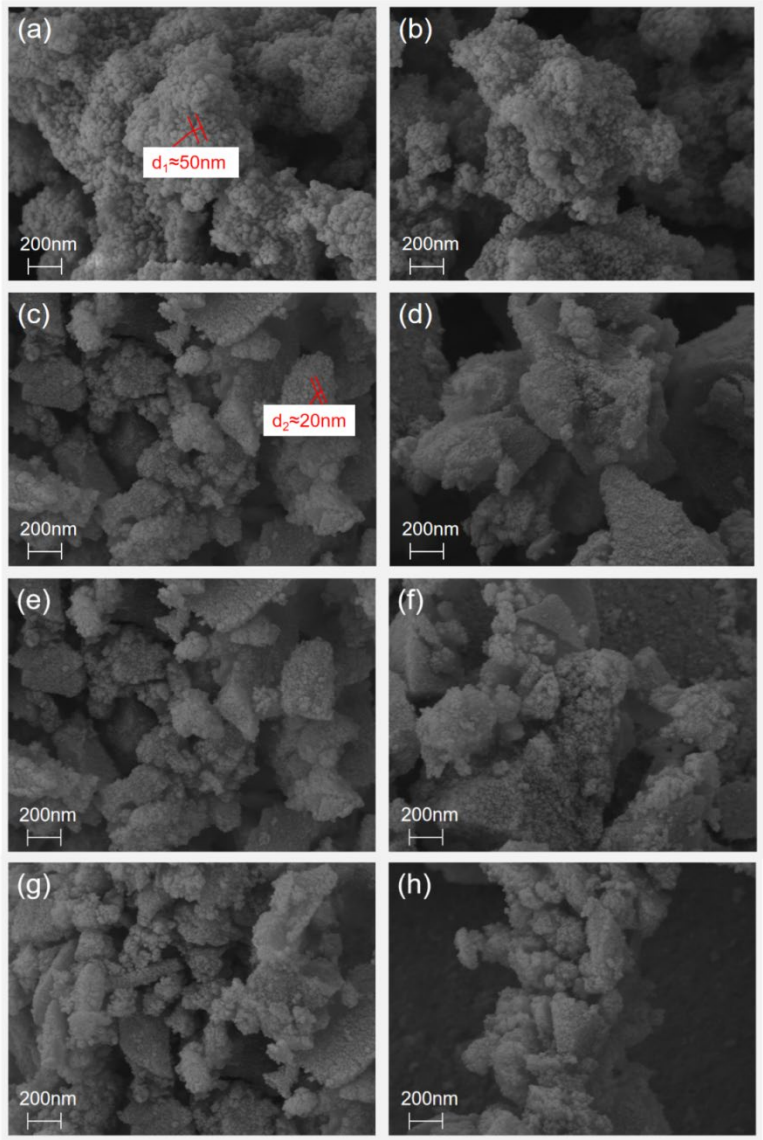

Figure 4: SEM, (a) TpH-7; (b)TpH-11.5; (c)TiO_2-7; (d)TiO_2-11.5.(e)Fe(0%)-TiO_2; (f)Fe(0.5%) -TiO_2; (g)Fe(0.5%)-TiO_2; (h)Fe(0.5%)TiO_2-11.5.

3.1.2. EDS

Figure 5 shows the EDS spectrum of Fe (0.5%) - TiO_2 sample. Figure 5(a) shows the electronic image of the EDS sample. Draw any area from the field of view of the electronic image as the scanning area of the EDS test. Figure 5(b) shows the total spectrum of EDS surface. It can be seen from Figure 5(b) that the spectrum contains three elements, namely, Ti, O and Fe, which indicates that the sample contains not only the Ti and O elements of TiO_2 itself, but also the Fe element; It can be seen from the element content table in Figure 5(c) that the content of Fe accounts for 2.45% of the total content of all elements in the scanning area. It can be inferred that the content of Fe in the sample is in a reasonable range relative to the amount of Fe doping in the sample.

ISSN 2616-5880 Vol. 4, Issue 3: 1-14, DOI: 10.25236/AJMC.2023.040301

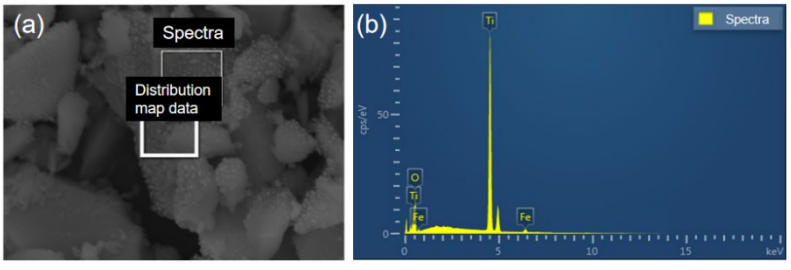

(c)

Element	Linetype	Apparentconcentration	K-ratio	wt%	wt% Sigma	Atomicpercentage	StandardSamplelabels
O	K	22.21	0.075	24.10	0.20	51.04	SiO_2
Ti	K	137.54	1.375	65.09	0.20	46.04	Ti
Fe	K	4.900	0.049	2.45	0.08	1.49	Fe
Total				100.00		100.00	

(d)

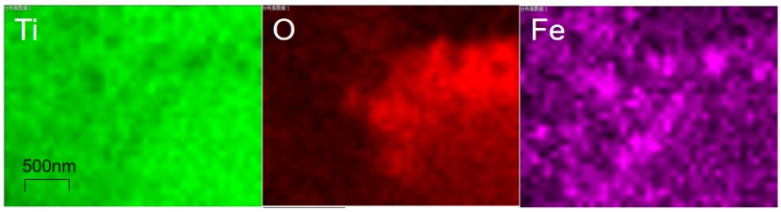

Figure 5: EDS spectrum of Fe (0.5%) TiO_2-11.5, (a) EDS electronic image; (b) EDS surface total spectrum; (c) Element content table; (d) EDS atlas element distribution diagram (Ti, O, Fe elements).

Combined with the element distribution diagram in Figure 5(d), it can be seen that the distribution of Fe element in the scanned area is relatively uniform, indicating that the distribution of Fe element in the sample is relatively uniform. Therefore, it is speculated that Fe is successfully doped into self-made TiO_2, which will be further confirmed by other relevant characterization.

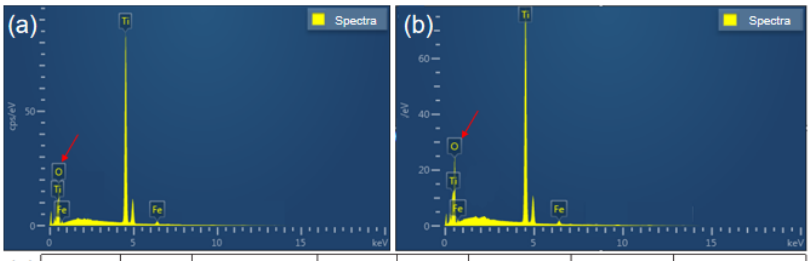

(c)

Element	Linetype	Apparentconcentration	K-ratio	wt%	wt% Sigma	Atomicpercentage	StandardSamplelabels
O	K	22.21	0.075	24.10	0.20	51.04	SiO_2
Ti	K	137.54	1.375	65.09	0.20	46.04	Ti
Fe	K	4.900	0.049	2.45	0.08	1.49	Fe
Total				100.00		100.00	

(d)

Element	Linetype	Apparentconcentration	K-ratio	wt%	wt% Sigma	Atomicpercentage	StandardSamplelabels
O	K	28.74	0.097	28.19	0.19	56.90	SiO_2
Ti	K	127.52	1.275	59.56	0.19	40.16	Ti
Fe	K	4.62	0.043	2.26	0.07	1.31	Fe
Total				100.00		100.00	

Figure 6: Comparison diagram of atomic percentage of O element of Fe (0.5%)-TiO_2 and Fe (0.5%) TiO_2-11.5, (a) total spectrum of Fe (0.5%)-TiO_2; (b) Total spectrum of Fe (0.5%) TiO_2 2-11.5 surface; (c) EDS element content of Fe (0.5%)-TiO_2; (d) EDS element content of Fe (0.5%) TiO_2-11.5.

Figure 6 shows the comparison of the atomic percentage of O element between Fe (0.5%)-TiO_2 and Fe (0.5%)TiO_2-11.5. The comparison between Figure 6(a) and figure b shows that the concentration of O in figure a is lower than that in Figure 6(b); Combined with the Figure 6(c) diagram and Figure 6(d) diagram, the atomic percentage of O element in the c diagram is 51.04%, which is lower than the atomic percentage of O element in the d diagram (56.90%). This shows that the atomic percentage of O element in the sample is higher after the surface modification of alkali solution. The reason for this difference may be that the content of OH^- adsorbed in the alkali solution is very high, which is

ISSN 2616-5880 Vol. 4, Issue 3: 1-14, DOI: 10.25236/AJMC.2023.040301

adsorbed on the surface of the sample [10] during the impregnation process, resulting in an increase in the content of O element. Therefore, the atomic percentage of O element of Fe (0.5%) TiO_2-11.5 is higher than that of Fe (0.5%) - TiO_2.

3.1.3. X-ray diffraction (XRD)

Figure 7(a) is the XRD spectrum of commercial TiO_2 modified by alkali solution surface. The typical characteristic peak of anatase is at 25.6 ° [11]. It can be judged by comparing the standard card of TiO_2 that the sample is TiO_2. After the surface modification of alkali solution, since each diffraction peak does not shift and no other impurity peaks appear, it can be inferred that the surface modification of alkali solution does not affect the crystal structure of commercial TiO_2.

Figure 7(b) is the XRD pattern of self-made TiO_2 modified by alkali solution surface. Compared with Figure a, it can be seen that the diffraction peak characteristics of this sample and commercial TiO_2 are not different, so it can be determined that self-made TiO_2 has been successfully prepared, and the crystal structure has not changed after alkali solution modification.

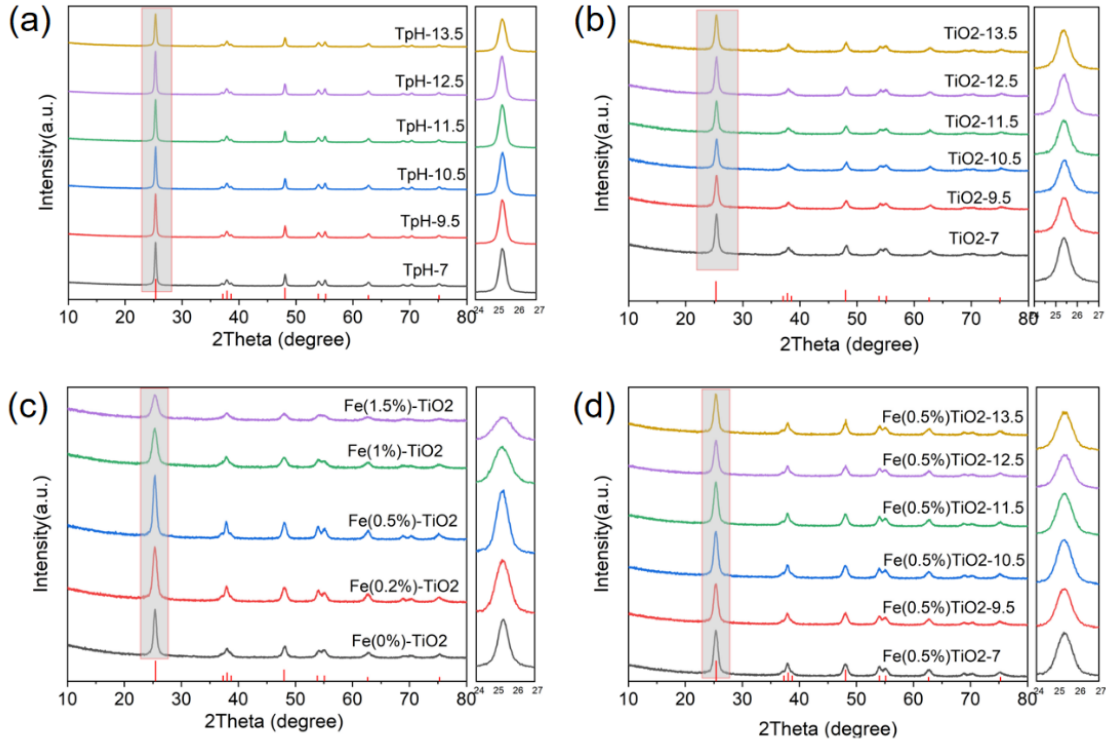

Figure 7: XRD test pattern, (a) surface modification of commercial TiO_2 with different pH alkali solutions; (b) Surface modification of self-made TiO_2 with alkali solution of different pH; (c) Fe-doped self-made TiO_2 with different Fe-doped amounts; (d) Surface modification of Fe (0.5%) TiO_2 in alkaline solution with different pH.

Figure 7(c) shows the XRD pattern of Fe-doped TiO_2. When the doping amount of Fe gradually increases from 0 to 0.5%, the characteristic peaks and other diffraction peaks of the sample gradually become stronger, which indicates that the crystallinity of the sample is enhanced. When the doping amount of Fe gradually increases from 0.5% to 1.5%, the characteristic peak and other diffraction peaks gradually weaken. As the crystallinity is better, the defects of titanium dioxide nanoparticles are more and the particle size is smaller, so the number of particles per unit mass is more and the specific surface area is larger. On the one hand, the larger the specific surface area, the stronger the ability of adsorbing reactants and receiving light, and the more active sites per unit area; On the other hand, the more titanium dioxide defects, the higher the transfer efficiency of photogenerated carriers [12]. It can be concluded that the photocatalytic performance of Fe-doped TiO_2 is better than that of undoped TiO_2, and the photocatalytic performance is the best when the amount of Fe-doped is 0.5%. No obvious Fe ion diffraction peak can be observed in Figure 7(c). The reason may be: on the one hand, the radius of Fe ion is larger than that of Ti ion, resulting in a very small amount of Fe ion can only be dispersed in the lattice gap of TiO_2, but cannot enter the lattice of TiO_2; On the other hand, the doping amount of Fe is very low, resulting in a very low content of Fe ions in the sample [13], so no obvious diffraction peak

ISSN 2616-5880 Vol. 4, Issue 3: 1-14, DOI: 10.25236/AJMC.2023.040301

can be formed.

Figure 7(d) shows the XRD pattern of the surface modification of the alkaline solution with Fe-doped TiO_2. Compared with the pattern of the sample before the modification and the TiO2 standard card, it can be seen that the surface modification of the alkaline solution will not affect the crystal structure of Fe (0.5%) - TiO_2.

3.1.4. Fourier transform infrared spectroscopy (FT-IR)

Figure 8 shows Fourier Transform Infrared Spectroscopy (FT-IR). Figure 8(a) shows the analysis and comparison of commercial TiO_2 and self-made TiO_2 samples before and after surface modification of alkali solution. Both TpH-7 and TpH-11.5 have an obvious absorption peak at 551cm^{-1}, corresponding to the characteristic peak of TiO_2 [14]; The corresponding peak at 1633cm^{-1} and 3433cm^{-1} is OH▪ (hydroxy), which is due to the fact that TiO_2 itself contains a small amount of OH▪. It shows that commercial TiO_2 does not introduce other organic substances or functional groups before and after surface modification of alkali solution. TiO_2-7 and TiO_2-11.5 also have characteristic peaks of TiO_2 at 500cm^{-1}, but the positions of the peaks shift relative to TpH-7 and TpH-11.5. This is because TiO_2-7 and TiO_2-11.5 are prepared by using raw materials such as tetrabutyl titanate. The preparation process uses a relatively short calcination time and a relatively mild calcination temperature, so the crystallinity of the product is relatively low and has more defects, so the position of the characteristic peak shifts.

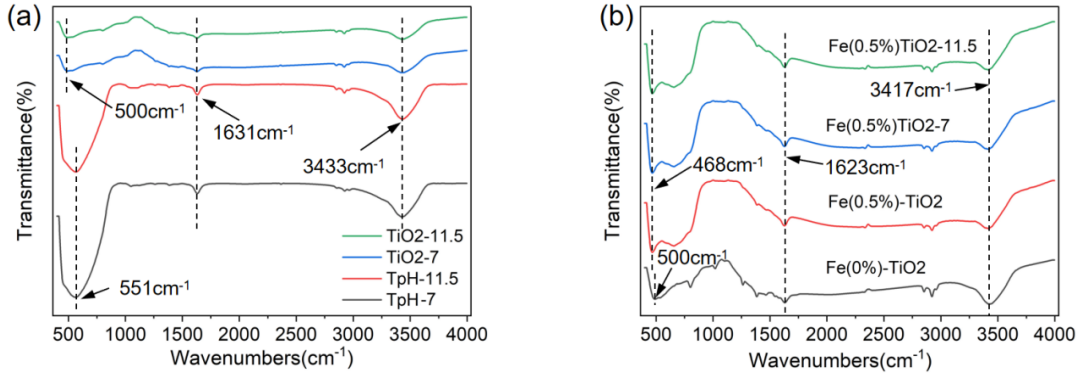

Figure 8: FT-IR spectrum, (a) before and after surface modification of commercial TiO2 and self-made TiO2 alkaline solution; (b) Before and after surface modification of Fe (0.5%) - TiO2 with Fe-doped TiO2 and alkali solution.

Figure 8(b) shows the FT-IR spectra of Fe-doped TiO_2 and its alkali solution before and after surface modification. Fe (0%) TiO_2-7 corresponds to the characteristic peak of TiO_2 at 500cm^{-1}, and OH▪ at 1623cm^{-1} and 3417cm^{-1} (hydroxy), which is also due to the small amount of OH▪ carried by TiO_2 itself. The characteristic peak of Fe (0.5%) - TiO_2 is located at 468cm^{-1}, and the position of the characteristic peak shifts relative to Fe (0%) TiO_2 - 7. This may be due to lattice distortion or defects of TiO_2 crystal structure caused by Fe doping modification. TiO_2 characteristic peak and OH in Fe (0.5%) TiO_2-7 and Fe (0.5%) TiO_2-11.5 samples ▪ There is no deviation, which means that the surface modification of alkali solution will not change the crystal structure of the sample and will not introduce other organic substances or functional groups [15].

3.1.5. X-ray photoelectron spectroscopy (XPS)

Figure 9 is the XPS test spectrum of Fe (0.5%) - TiO_2 sample. Figure 9(a) shows the presence of Ti, O, Fe and C elements, which are mainly the standard correction peak of the instrument and are used to calibrate the binding energy position. In addition, it may also be carbon impurities in sample Fe (0.5%) - TiO_2 or carbon dioxide absorbed in the air.

ISSN 2616-5880 Vol. 4, Issue 3: 1-14, DOI: 10.25236/AJMC.2023.040301

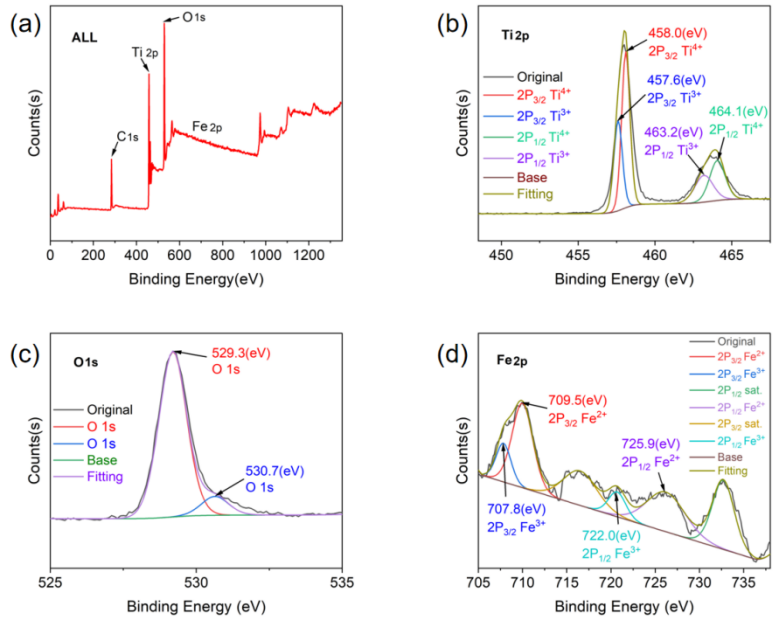

Figure 9: X-ray photoelectron spectrum of Fe (0.5%) - TiO_2, (a) XPS full spectrum; (b)Fe 2p; (c)Ti 2p; (d)O 1s.

Figure 9(b) is the high-resolution spectrum of Ti 2p. It can be seen that the Fe (0.5%) - TiO_2 sample has four fitting peaks, Ti 2p3/2 peak at 458.0eV, Ti 2p1/2 peak at 464.1eV, and the binding energy distance is 6.1eV, which proves that Ti in the sample mainly exists in the form of tetravalent Ti ion (Ti^{4+}). In addition, there are two peaks at 457.6eV and 463.2eV, which are offset from the peaks at 458.0eV and 464.1eV, indicating that there are also trivalent Ti ions (Ti^{3+}) in the sample [16]. There are many reasons for producing Ti^{3+}ions. First, when Fe ions enter TiO_2 through doping, the TiO_2 particles generate oxygen vacancies, thus producing Ti^{3+}ions. In addition, there are a few hydroxyl groups on the surface of TiO_2 particles, which generate Ti^{3+}ions during the photocatalytic reaction. Since the surface state of $Ti^{3+}$is only 0.3eV from the bottom of the conduction band of TiO_2, it can effectively capture the e^- generated by the conduction band in the photocatalytic reaction, which to some extent inhibits the recombination probability of photogenerated electron holes, thus improving the photocatalytic performance.

Figure 9(c) shows the high-resolution spectrum of O 1s. The results show that O 1s has two fitting peaks, located at 529.3eV and 530.7eV respectively, where 529.3eV corresponds to lattice oxygen and 530.7eV corresponds to adsorbed oxygen [17]. Lattice oxygen comes from O in the TiO_2 lattice, and adsorbed oxygen may come from oxygen-containing substances such as water molecules on the sample surface.

Figure 9(d) shows the high-resolution spectrum of Fe 2p. It shows that there are two peaks of Fe at 707.8eV and 720.6eV, both of which are positive trivalent Fe. The peaks at 709.9eV and 725.9eV have shifted compared with the first two peaks, indicating that there is still positive divalent Fe in the Fe ion. As shown in Table 1, the calculated percentage of Fe/TiO_2 is 1.13%, which indicates that the concentration of Fe doping in the sample is 1.13% [18].

Table 1 Element Concentration Table

Name	Peak BE	FWHM eV	Area(P) CPS.eV	Atomic %
Ti2p	458.02	2.67	375086.84	17.23
O1s	529.25	2.73	341521.42	43.58
C1s	284.01	2.75	112474.18	38.50
Fe2p1/2	721.96	2.87	6348.21	0.46
Fe2p3/2	709.54	0.96	6001.75	0.23

ISSN 2616-5880 Vol. 4, Issue 3: 1-14, DOI: 10.25236/AJMC.2023.040301

3.2. Photocatalytic performance

3.2.1. Photocatalytic performance of commercial TiO_2 surface modified by alkali solution

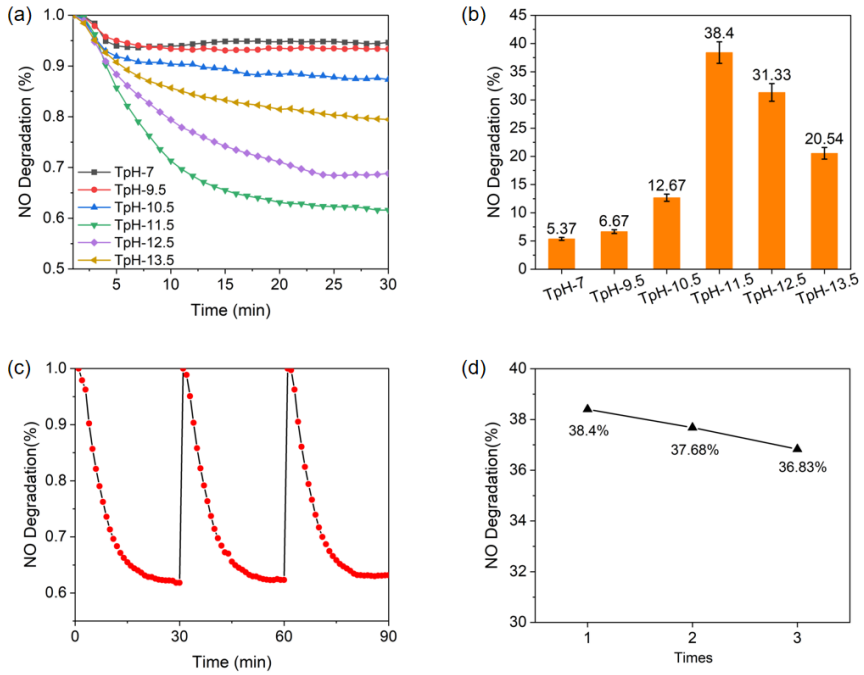

Figure. 10: Nitrogen-oxygen catalytic test of commercial TiO_2 under different alkalinity modifications, (a) Nitrogen-oxygen catalytic test of NO degradation rate; (b) Histogram of NO degradation rate; (c) Nitrogen and oxygen catalytic cycle test of TpH-11.5; (d) Nitrogen and oxygen catalytic cycle test of TpH-11.5 for NO degradation rate.

As shown in Figure 10(a) (b), the degradation rate of NO (nitric oxide) in the TpH-7 control group without alkali solution modification of commercial TiO_2 is only 5.37%; However, after surface modification of alkali solution with different pH values, the NO degradation ability of each experimental group was improved to different degrees. When the pH was 11.5 (TpH-11.5 group), the NO degradation rate reached the highest (38.4%), which was 33.03% higher than that of TpH-7 control group, and the NO degradation rate of other experimental groups was also improved to different degrees. This may be because the hydroxide ion in the alkali solution is attached to the TiO_2 surface [19]. When the photocatalysis reaction is carried out, the hydroxide ion on the modified TiO_2 surface is oxidized to hydroxyl radical (OH ·) by the hole (h^+), thus enhancing the photocatalysis performance, which also fully proves that the surface modification of the alkali solution is very effective for improving the photocatalysis performance of TiO_2. When the pH value of the alkali solution increased from 7 to 11.5, the NO degradation rate of the experimental group showed an upward trend; When it exceeds 11.5, the degradation rate of NO tends to decline. This may be because when the pH value of the alkali solution is too low, the number of hydroxide ions in the alkali solution is too small to maximize the photocatalytic performance; When the pH value of the alkali solution is too large, the number of hydroxide ions is too large, so that some hydroxide ions occupy the active sites [20], affecting the separation of photogenerated electron hole pairs.

Figure 10(c) (d) is the broken line diagram of the NO degradation rate of the nitrogen-oxygen catalytic cycle test and the nitrogen-oxygen catalytic cycle test of TpH-11.5 group samples. It can be found that after three cycles of test on the samples of TpH-11.5 group with the best photocatalytic performance in the experimental group, the degradation rate of NO in each cycle test is 38.4%, 37.68% and 36.83%, respectively. After three cycles, the degradation rate of NO is about 4.09%. This shows that the surface modification of commercial TiO_2 with alkali solution is recyclable.

3.2.2. Photocatalytic performance of self-made TiO_2 modified on the surface of alkali solution

As shown in Figure 11(a)(b), TiO_2-7 group samples are self-made TiO_2 without surface modification of alkali solution, and its NO degradation rate is 30.96%, which is significantly higher than that of commercial TiO_2 without surface modification of alkali solution (section 3.4.1, TpH-7 group samples) (5.37%). This shows that the photocatalytic performance of self-made TiO_2 is far better

ISSN 2616-5880 Vol. 4, Issue 3: 1-14, DOI: 10.25236/AJMC.2023.040301

than that of commercial TiO_2. The reason may be that the preparation conditions of self-made TiO_2 are conducive to the formation of larger specific surface area and more defects, thus improving the light absorption ability and photocatalytic performance. After surface modification of self-made TiO_2 with alkali solution of different pH, the NO degradation rate of samples in each experimental group has been improved to a certain extent, among which, when the pH of alkali solution is 11.5 (TiO_2-11.5 group samples), the NO degradation rate is the highest (46.81%), which is 15.85% higher than the control group (TiO_2-7 group samples); Compared with commercial TiO_2 modified by alkali solution under the same conditions, the NO degradation rate of self-made TiO_2 modified by alkali solution is 8.41% higher. This also shows that the photocatalytic performance of self-made TiO_2 before and after modification is better than that of commercial TiO_2.

As shown in Figure 11(c)(d), in order to study the stability and recyclability of the photocatalytic performance of self-made TiO_2 after surface modification by alkali solution, the nitrogen-oxygen catalytic cycling test was still carried out for the group with the highest NO degradation rate (TiO_2-11.5 group) in the experimental group. The NO degradation rate was 46.81%, 46.35% and 45.92% in the cyclic test, respectively. After the cycling test, the degradation rate of NO degradation capacity accounted for about 1.90%. This shows that its circularity is excellent.

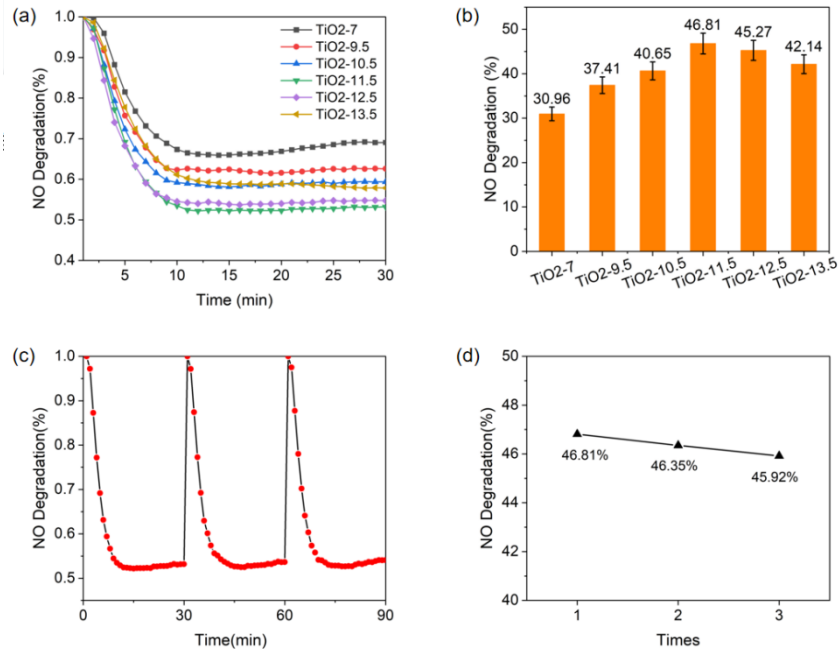

Figure. 11: Nitrogen-oxygen catalytic test of self-made TiO_2 under different alkalinity modification, (a) Nitrogen-oxygen catalytic test of NO degradation rate; (b) Histogram of NO degradation rate; (c) Nitrogen and oxygen catalytic cycle test of TiO_2-11.5; (d) NO degradation rate broken line diagram of TiO_2 - 11.5 nitrogen and oxygen catalytic cycle test.

3.2.3. Photocatalytic performance of Fe-doped TiO_2

As shown in Figure 12(a) (b), the NO degradation rate of each experimental group was improved after the self-made TiO_2 was doped with different doping ratios. When the doping ratio was Fe/Ti=0.5% (Fe (0.5%) - TiO_2 group), the NO degradation rate increased to the highest value of 47.6%. Compared with pure self-made TiO2, its NO degradation rate increased by 16.64%, and other doping amount experimental groups also increased to a certain extent. This may be because the radius of Fe ion is similar to that of Ti ion, and Fe ion replaces the position of Ti4+by doping, thus narrowing the band gap of TiO_2 [21]; At the same time, the appropriate doping ratio can make Fe ions form a certain number of shallow potential traps in TiO_2, making the surface activity higher [22], and can effectively capture photogenerated electron holes, so that the electron hole pairs can be effectively separated. It can also be seen from the figure that when the doping ratio increases from 0 to 0.5%, the NO degradation rate of the experimental group shows an upward trend; When it exceeds 0.5%, it turns into a downward trend. This is because when the doping ratio is too small, the number of shallow potential wells used to capture the electron hole pairs is insufficient, resulting in the failure of effective separation of some electron hole pairs, thus limiting the space for improving the photocatalytic performance; However, when the doping ratio is too large, local agglomeration will easily occur, affecting the conductivity, and

ISSN 2616-5880 Vol. 4, Issue 3: 1-14, DOI: 10.25236/AJMC.2023.040301

the average spacing between capture sites will be too small, which will greatly increase the recombination rate of electron holes, thus inhibiting the photocatalytic performance.

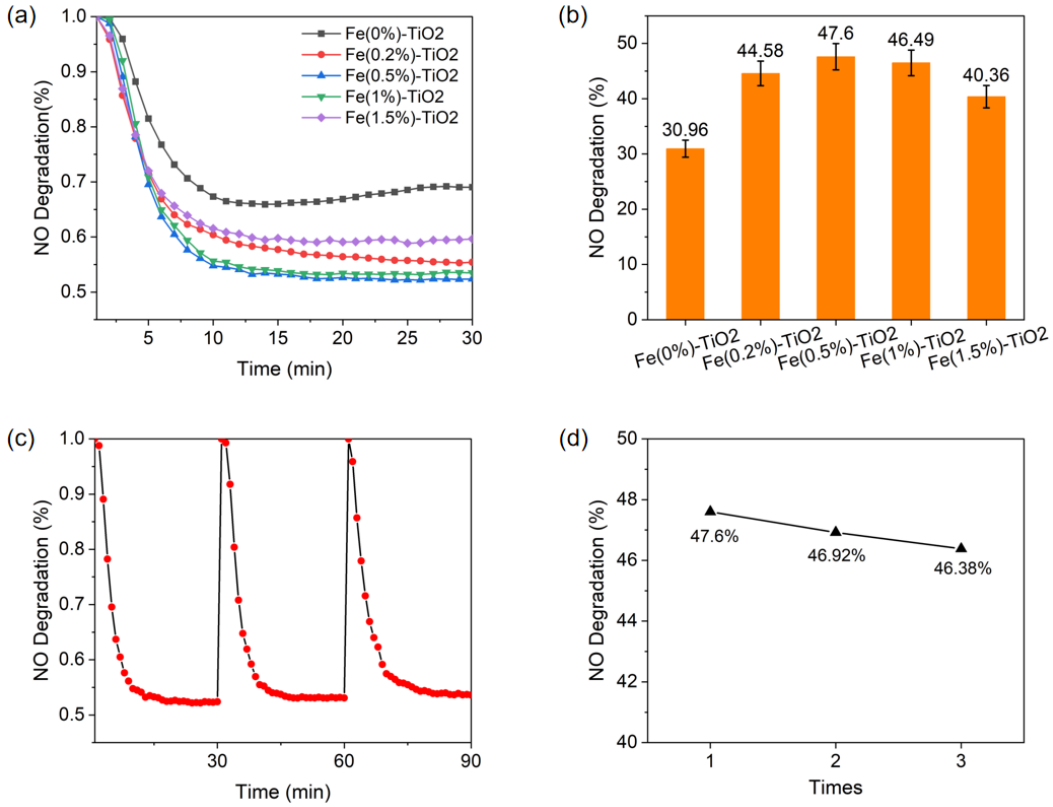

Figure 12: Nitrogen-oxygen catalytic test of Fe-doped TiO_2 under different doping ratios, (a) Nitrogen-oxygen catalytic test of NO degradation rate; (b) Histogram of NO degradation rate; (c) Nitrogen and oxygen catalytic cycle test of Fe (0.5%) - TiO_2; (d) NO degradation rate broken line diagram of Fe (0.5%) - TiO_2 nitrogen and oxygen catalytic cycle test.

Figure 12(c) (d) shows the nitrogen-oxygen catalytic cycle test of the best performance experimental group Fe (0.5%) - TiO_2. It can be seen that the NO degradation trend of the single cycle is the same, with the NO degradation rate of 47.6%, 46.92% and 46.38% respectively. After the three cycle tests, the NO degradation ability decreases by about 2.56%, indicating that it has excellent cycle stability.

3.2.4. Photocatalytic performance of Fe-TiO_2 surface modified by alkali solution

It can be seen from Figure 13(a)(b) that in the experimental group with the best NO degradation rate of Fe-doped TiO_2 (Fe (0.5%) - TiO_2 group), after surface modification of alkali solution with different pH values, the NO degradation rate of each experimental group has been improved to varying degrees. When the pH of the alkali solution is 11.5 (Fe (0.5%) TiO_2-11.5 group), the NO degradation rate is 53.83%, which is 6.23% higher than that of Fe (0.5%) - TiO_2 without surface modification of the alkali solution. The reason may be that when photocatalysis reaction is carried out, on the one hand, when Fe ion replaces Ti^{4+}, TiO_2 will generate a new energy level, resulting in a narrow band gap, thus extending the light response range to visible light. At the same time, as a shallow potential trap, Fe ion can enhance the separation efficiency of its photogenerated electron hole; On the other hand, the alkali solution provides the maximum number of hydroxide ions for the photocatalyst, making it produce sufficient hydroxyl radicals after being oxidized by photogenic holes, thus improving the photocatalytic performance.

ISSN 2616-5880 Vol. 4, Issue 3: 1-14, DOI: 10.25236/AJMC.2023.040301

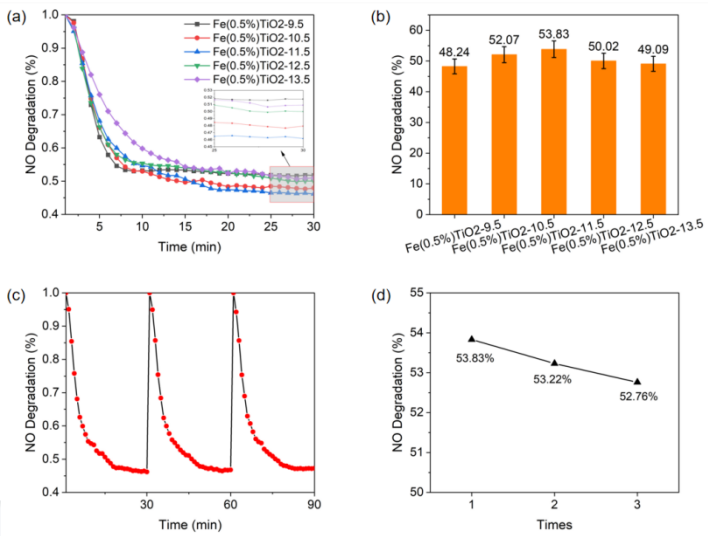

Figure 13: Nitrogen-oxygen catalytic test of Fe (0.5%) - TiO_2 under different alkalinity modification, (a) Nitrogen-oxygen catalytic test of NO degradation rate; (b) Histogram of NO degradation rate; (c) Nitrogen and oxygen catalytic cycle test of Fe (0.5%) TiO_2-11.5; (d) NO degradation rate broken line diagram of nitrogen and oxygen catalytic cycle test for Fe (0.5%) TiO_2-11.5.

Figure 13(c) (d) shows the nitrogen-oxygen catalytic cycle test of Fe (0.5%) TiO_2-11.5 group samples. In the cycle test, the NO degradation rate of a single cycle is 53.83%, 53.22% and 52.76% respectively, and the decline of the NO degradation rate is about 1.99%, with good recyclability and stability.

4. Conclusions

In order to improve the photocatalytic performance of commercial TiO_2 and self-made TiO_2, the following work has been carried out in this chapter: surface modification of commercial TiO_2 in alkaline solution; Self-made TiO_2 was prepared by sol gel method and optimized process; The surface of self-made TiO_2 was modified by alkali solution; The self-made TiO_2 was modified by iron doping; The surface of Fe-doped TiO_2 was modified by alkali solution; The morphology, crystal phase, structure and element composition of the modified TiO_2 were analyzed by microscopic characterization test; The photocatalytic performance of various products was evaluated by nitrogen and oxygen catalytic test and NO degradation rate; The enhancement mechanism of photocatalytic performance of modified TiO_2 was analyzed. The following conclusions are drawn from the above work:

(1) After the commercial TiO_2 was modified by alkali solution surface modification, the photocatalytic performance was improved to varying degrees, and the NO degradation rate of TpH-11.5 group samples reached 38.4%, while the NO degradation rate of the unmodified TpH-7 group samples was only 5.37%. The NO degradation rate of self-made TiO_2 before modification (TiO_2-7 samples) was 30.96%. After surface modification by alkali solution, the photocatalytic performance also improved, and the NO degradation rate of TiO_2-11.5 samples increased to 46.81%. It can also be found that the photocatalytic performance of self-made TiO_2before and after surface modification of alkali solution is better than that of commercial TiO_2.

(2) In the process of preparing TiO_2 by the sol gel method, TiO_2 was modified by Fe doping, which significantly improved the photocatalytic performance of self-made TiO_2. The NO degradation rate of self-made TiO_2 without Fe doping modification (Fe (0%) - TiO_2 group) is 30.96%. When doped with 0.5% Ti/Fe molar ratio, the NO degradation rate of Fe (0.5%) - TiO_2 group is up to 47.6%.

(3) The surface modification of self-made TiO_2 (Fe (0.5%) - TiO_2 group) doped with Fe with the best photocatalytic performance was carried out in alkaline solution, and its photocatalytic performance was enhanced. Among them, when the pH value of the alkali solution is 11.5, the photocatalysis performance has the greatest improvement, and the NO degradation rate of Fe (0.5%) TiO_2-11.5 group samples has increased from 47.6% to 53.83%.

(4) In the surface modification of alkali solution, the optimal pH value of alkali solution is 11.5. Lower or higher than this value will make the photocatalytic performance of modified TiO_2 unable to

ISSN 2616-5880 Vol. 4, Issue 3: 1-14, DOI: 10.25236/AJMC.2023.040301

be improved to the maximum extent.

References

[1] Jones E R, Bierkens M F P, Wanders N, et al. Current wastewater treatment targets are insufficient to protect surface water quality[J]. Communications Earth & Environment, 2022, 3(1): 221.
[2] Rudke A P, Martins J A, Hallak R, et al. Evaluating TROPOMI and MODIS performance to capture the dynamic of air pollution in São Paulo state: A case study during the COVID-19 outbreak[J]. Remote Sensing of Environment, 2023, 289: 113514.
[3] Pozzer A, Anenberg S C, Dey S, et al. Mortality attributable to ambient air pollution: A review of global estimates[J]. GeoHealth, 2023: e2022GH000711.
[4] Jayranjan M, Eskinder G, Amit K. The development of techno-economic assessment models for hydrogen production via photocatalytic water splitting [J]. Energy Conversion and Manage ment, 2023, 279: 116750.
[5] Yongjun S, Yunli W, Yin C, et al. Synthesis of Fe3O4/CuO/ZnO/RGO and its catalytic degradation of dye wastewater using dielectric barrier discharge plasma [J]. Arabian Journal of Chemistry, 2023, 16(4): 104571.
[6] Keun S K, Min S J, Sungwoo K, et al. Singlet-oxygen-driven photocatalytic degradation of gaseous formaldehyde and its mechanistic study[J]. Applied Catalysis B: Environmental, 2023, 328: 122463.
[7] Wang J, Ma R, Jiang Z. The preparation of dodecyl trimethyl ammonium bromide modified titanium dioxide for the removal of uranium[J]. Environmental Science and Pollution Research, 2022: 1-9.
[8] Jia H, Dong M, Yuan Z, et al. Deep eutectic solvent electrolysis for preparing N and P co-doped titanium dioxide for rapid photodegradation of dyestuff and antibiotic[J]. Ceramics International, 2021, 47(16): 23249-23258.
[9] Salomatina E V, Fukina D G, Koryagin A V, et al. Preparation and photocatalytic properties of titanium dioxide modified with gold or silver nanoparticles[J]. Journal of Environmental Chemical Engineering, 2021, 9(5): 106078.
[10] Xin Y, Sun B, Liu J, et al. Effects of electrode configurations, solution pH, TiO2 addition on hydrogen production by in-liquid discharge plasma [J]. Renewable Energy, 2021, 171: 728-734.
[11] Mancuso A, Sacco O, Vaiano V, et al. Visible light active Fe-Pr co-doped TiO2 for water pollutants degradation[J]. Catalysis Today, 2021, 380: 93-104.
[12] Yoon S H, ElShorafa R, Katbeh M, et al. Effect of shape-driven intrinsic surface defects on photocatalytic activities of titanium dioxide in environmental application [J]. Applied Surface Science, 2017, 423: 71-77.
[13] Zouheir M, Tanji K, Navio J A, et al. Effective photocatalytic conversion of formic acid using iron, copper and sulphate doped TiO_2[J]. Journal of Central South University, 2022, 29(11): 3592-3607.
[14] Sarker D R, Uddin M N, Elias M, et al. P-doped TiO_2-MWCNTs nanocomposite thin films with enhanced photocatalytic activity under visible light exposure [J]. Cleaner Engineering and Technology, 2022, 6: 100364.
[15] Mugundan S, Praveen P, Sridhar S, et al. Sol-gel synthesized barium doped TiO2 nanoparticles for solar photocatalytic application[J]. Inorganic Chemistry Communications, 2022, 139.
[16] Zhu J, Wu D, Liang P, et al. Ag+/W6+ co-doped TiO2 ceramic with colossal permittivity and low loss [J]. Journal of Alloys and Compounds, 2021, 856: 157350.
[17] Wang Y, Chen J, Zhang X, et al. N-doped rutile TiO2/C hybrids with enhanced charge transfer capability derived from NH2-MIL-125 (Ti) for the photocatalytic degradation of tetracycline [J]. Materials Research Bulletin, 2022, 155: 111968.
[18] Zouheir M, Tanji K, Navio J A, et al. Effective photocatalytic conversion of formic acid using iron, copper and sulphate doped TiO_2[J]. Journal of Central South University, 2022, 29(11).
[19] Zhou K L, Wang Z, Han C B, et al. Platinum single-atom catalyst coupled with transition metal/metal oxide heterostructure for accelerating alkaline hydrogen evolution reaction[J]. Nature Communications, 2021, 12(1): 3783.
[20] Yu H, Jing Y, Du C F, et al. Tuning the reversible chemisorption of hydroxyl ions to promote the electrocatalysis on ultrathin metal-organic framework nanosheets[J]. Journal of Energy Chemistry, 2022, 65: 71-77.
[21] Zeng Z, Xu M, Sun Y, et al. First-principles study on the optical spectrum of N/P doped TiO2-anatase [J]. Optik, 2022, 261: 169231.
[22] Dong S, Chen S, He F, et al. Construction of a novel N-doped oxygen vacancy-rich TiO2 N-TiO2−X/g-C3N4 S-scheme heterostructure for visible light driven photocatalytic degradati on of 2, 4-dinitrophenylhydrazine[J]. Journal of Alloys and Compounds, 2022, 908: 164586.